Processing and Application of Ceramics 19 [2] (2025) 150–156
https://doi.org/10.2298/

The influence of solvent and number of layers on the homogeneity and properties of ZnO thin films obtained by spin-coating method

Almedina Modrić-Šahbazović[1,*], Zerina Sakić[1], Maja Đekić[2], Senad Isaković[2], Izet Gazdić[1]

[1]*Department of Physics, Faculty of Natural Sciences and Mathematics, University of Tuzla, 75000 Tuzla, Bosnia and Herzegovina*
[2]*Department of Physics, Faculty of Natural Sciences and Mathematics, University of Sarajevo, 71000 Sarajevo, Bosnia and Herzegovina*

Received 28 February 2025; Received in revised form 19 May 2025; Accepted 8 June 2025

Abstract

Homogeneous semiconducting ZnO thin films were successfully produced using spin-coating method. The influence of structure and morphological properties of three-layered and five-layered ZnO films, made with different solvents (methanol and 2-methoxyethanol), on the band gap width was investigated. Scanning electron microscopy and atomic force microscopy analyses clearly showed the wrinkled surface of the ZnO thin films grown from the methanol solution, while the films grown from the 2-methoxyethanol solution were much more homogeneous. X-ray diffraction analysis revealed the hexagonal wurtzite structure of the obtained ZnO films, with preferential crystal growth along the c-axis. As the number of layers increased, the diffraction peaks became sharper and more intense. The crystallite size was calculated to be a few nanometers and gradually increased with the number of layers regardless of the solvent type, although it was slightly smaller for the 2-methoxyethanol solvent. UV-Vis spectra analysis, using the Tauc formula, showed that as the number of layers increased, the band gap width decreased regardless of the solvent choice.

Keywords: *ZnO, films, spin-coating method, surface properties, optical properties*

I. Introduction

Zinc oxide (ZnO) is a highly attractive II-VI semiconductor due to its unique properties, such as a wide band gap (3.37 eV) and high exciton binding energy (60 meV) at room temperature [1–3]. ZnO thin films have a wide range of applications thanks to their superior optical and electrical properties. They are used in the production of solar cells, conductive gas sensors, piezoelectric converters, transparent conductive electrodes and as antibacterial and anticorrosive agents [4–6]. These applications depend on the material's morphology, which can be achieved through various techniques. Some of the techniques used for preparing ZnO thin films include RF magnetron sputtering [7], physical vapour deposition (PVD) [8], chemical vapour deposition (CVD) [9], spray pyrolysis [10], pulsed laser deposition [11] and the sol-gel technique [12]. Among them, the sol-gel technique combined with a spin-coater has gained significant attention due to its simple deposition process, easy control of chemical components and low-cost preparation for producing high-quality thin films [13]. However, many parameters affect the properties of the resulting films, including the concentration of zinc salt, solvent, drying and annealing temperature, number of layers applied, film withdrawal speed, nature of the substrate and others [14].

This paper is focused on the production of multilayer ZnO films and the comparison of the effects of two types of solvents (methanol and 2-methoxyethanol) on the topography, structural and optical properties of ZnO thin films. The effect of the number of applied layers on a microscope glass substrate on these properties was also investigated. The results of this research will help to define the optimal conditions for producing high-quality homogeneous thin films for potential applications such as solar cells and photocatalysis [15,16].

* Corresponding author: +387 35 320 860
e-mail: *almedina.modricsahbazovic@untz.ba*

II. Experimental

2.1. Synthesis procedure

Two ZnO solutions were prepared in such a way that zinc acetate dihydrate ($C_4H_6O_4Zn \cdot H_2O$) was dissolved in the solvents methanol (CH_3OH) and 2-methoxyethanol ($C_3H_8O_2$). Afterwards, a stabilizer, monoethanolamine (MEA), was added in a 1:1 ratio in both cases. The solutions were mixed using a magnetic stirrer for 2 h at a temperature of 60 °C. The prepared ZnO solutions were left to age for 48 h, after which they were ready for application on to microscope slides that had previously been cut to 1 cm × 1 cm dimensions and cleaned in acetone, ethanol and distilled water in an ultrasonic bath. After thorough cleaning, the substrates were dried using an air stream and placed on a holder (disk) of the spin coater (Model P-6708D, Specialty Coating Systems, Indianapolis, IN), where the solutions were applied using a micropipette. A single ZnO layer was obtained by rotating the spin coater disk in a three-step procedure: 10 s at 1000 rpm, 10 s at 1500 rpm, and 20 s at 2000 rpm. After a thin layer was obtained, it was dried in an oven at 150 °C for 15 min, after which the process of dripping, centrifuging and drying was repeated until three-layered or five-layered ZnO films were obtained. The resulting films were annealed in vacuum in the furnace Nabertherm R 50/250/13 for 1 h at the temperature of 500 °C. A large number of researchers use this specific annealing temperature, as it induces crystallization, which is reported by Aoun *et al.* [17]. The labels of the produced films, together with the deposition parameters are given in Table 1.

Table 1. The labels of the produced ZnO thin films, together with the deposition parameters

Film label	Solvent	Number of layers
ZnO3_m	methanol	3
ZnO5_m	methanol	5
ZnO3_2m	2-metoxyethanol	3
ZnO5_2m	2-metoxyethanol	5

2.2. Characterization

The obtained thin films were first analysed using scanning electron microscopy (SEM, model JEOL JSM-IT200) equipped with secondary electron detector (SED) and energy dispersive spectrometer (EDS) in order to determine the topography and composition of the samples. The samples were examined in high-vacuum mode using accelerating voltage of 15 kV. To further investigate the thickness of the ZnO films, cross-sectional SEM micrographs were acquired using SEM (FEI Scios2 Dual Beam System). Due to the non-conductive nature of the glass substrate, a thin gold coating was applied prior to imaging. The surface morphology (roughness and grain size) was determined using atomic force microscopy (AFM, model Nanosurf CoreAFM). The images were obtained in a tapping mode using Nanosurf DynAl tips with nominal frequency 190 kHz and nominal force constant 48 N/m. For structural investigations, an X-ray diffractometer (XRD), model Bruker D8 Advance, was used, employing the Kα line of copper as the incident radiation, with a wavelength of 0.15418 nm. The XRD patterns were recorded using 2θ scan type where the incidence angle ω was kept at 0.8° (grazing incidence). Data were acquired via Bruker's LYNEXEYE XE-T detector in the range from 20° to 80° with a step size 0.02°, counting time 1 s, tube voltage 40 kV and tube current 40 mA. To examine the optical properties of the obtained films, ultraviolet-visible spectroscopy (UV-Vis, model Perkin Elmer Lambda 365) was used with a wavelength range of 190–1100 nm and a spectral resolution of 0.5 nm.

III. Results and discussion

SEM micrographs at a magnification of 10000× of the three-layered and five-layered ZnO films with methanol and 2-methoxyethanol solvents are shown in Fig. 1. Cross-sectional SEM images of the films are shown in the corresponding insets. The films obtained from the methanol solution exhibit a wrinkled surface due to the specific mechanical and chemical interactions between methanol and the zinc precursor compounds during the deposition process. Many authors have reported on the formation of wrinkled ZnO thin films. According to Kwon *et al.* [18] the wrinkles form due to the relaxation of stress caused by removal of solvent during drying process. Methanol, being a simpler solvent, evaporates more quickly due to its lower boiling point, which can cause rapid dehydration and the formation of stress in the film. These stresses can lead to the formation of wrinkles on the surface of the film, as the film contracts and pulls during the drying and calcination process. Due to the presence of wrinkles, their thickness is difficult to determine with high accuracy; however, the average thickness of the three-layered ZnO films is approximately 360 nm, while that of the five-layered films is around 460 nm. On the other hand, the ZnO films grown from the 2-methoxyethanol solution show a much more homogeneous surface because 2-methoxyethanol has a higher molecular weight and evaporates slower than methanol. As a result, the deposition process is moderate and less localized stress occurs, allowing for a more uniform distribution of zinc on the film surface. Additionally, the larger molecules of 2-methoxyethanol can coordinate more effectively with the zinc oxide precursor compounds, creating a more stable and homogeneous network during deposition. The thickness of the resulting three-layered films is 80 nm, while that of the five-layered films is 120 nm. Furthermore, it is observed that as the number of layers increases, the amplitude of the wrinkles decreases. This can be attributed to the increased stiffness and stress distribution in thicker films, which reduces the formation of pronounced wrinkles. In thinner films, the localized stress is more concentrated, leading to deeper and more

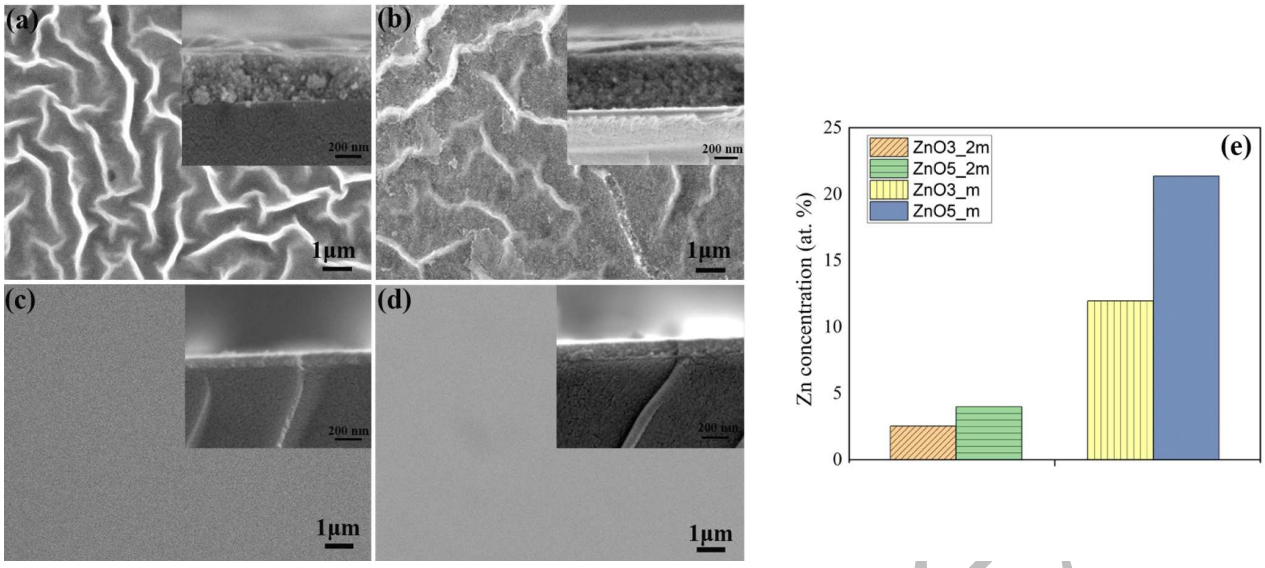

Figure 1. SEM micrographs with cross-section images shown in the insets of the three-layered (a) and five- layered (b) ZnO films prepared using methanol as the solvent, and the three- layered (c) and five- layered (d) ZnO films prepared using 2-methoxyethanol as the solvent, along with the zinc concentration in the ZnO films obtained from EDS spectra (e)

defined wrinkles. Thus, the increase in the number of layers results in a more uniform stress distribution, contributing to the reduction in the wrinkle depth.

An EDS analysis was also conducted, providing information on the atomic concentration of the elements present in the films. Besides Zn and O originating from the films, the analysis revealed the presence of Si and O coming from the glass substrates and some minor traces of C from the surface. The influence of the solvent and the number of layers on the Zn content is shown in Fig. 1e. Namely, the films produced from the solution with methanol solvent exhibit a significantly higher amount of zinc in comparison with the films obtained with 2-methoxyethanol solvent. In addition, amount of zinc increases with the number of layers, regardless of the used solvent. This also leads to the conclusion that, as the number of layers increases, the thickness of the films increases, which is consistent with the results obtained by Shariffudin *et al.* [19].

In addition to SEM, the topographical properties of the ZnO thin films were analysed using atomic force microscopy (AFM). Figure 2 shows the 2D AFM images of a part of the surface of ZnO thin films, with a 10 µm × 10 µm scan area. A mountainous (wavy) structure is clearly visible in the ZnO thin films obtained from the methanol-based solvent solution (Figs. 2a,b). The ZnO

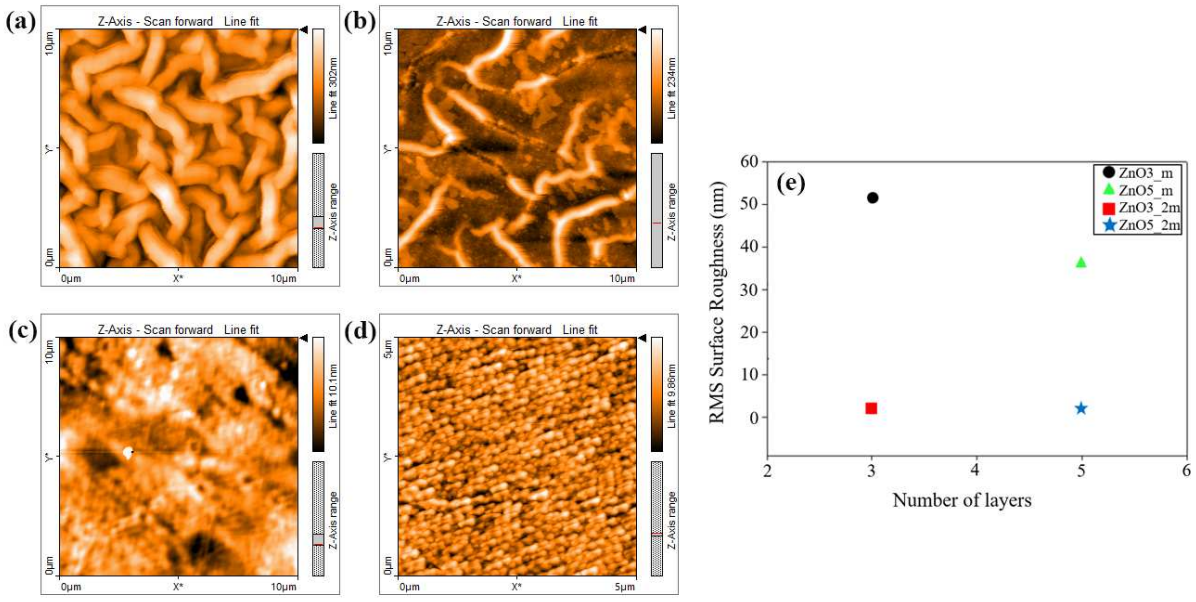

Figure 2. 2D AFM micrographs of three-layered (a) and five-layered (b) ZnO films with methanol solvent, and three-layered (c) and five-layered (d) ZnO films with 2-methoxyethanol solvent, as well as the surface roughness depending on the number of layers (e)

thin films produced with the 2-methoxyethanol solvent (Figs. 2c,d) display a much more homogeneous structure, which is in accordance with previously obtained SEM images. The roughness of the ZnO thin films decreases with increasing the number of layers, and its values are much higher for the films grown with methanol solvent compared to the 2-methoxyethanol solvent (Fig. 2e), which matches the data presented by Toubane *et al.* [20].

The structure of the ZnO films was examined using X-ray diffraction, and the recorded spectra are shown in Fig. 3. The obtained diffractograms confirm the hexagonal wurtzite structure (standard card for ZnO ICDD 36-1451), with matching diffraction peaks (100), (002), (101), (102), (110), (103) and (112) at precisely defined diffraction angles [21], which is shown in detail in Fig. 3. The films grown with methanol (Figs. 3a,b) display more intense peaks than the films grown with 2-methoxyethanol (Figs. 3c,d). Furthermore, (100), (002) and (101) peaks in Figs. 3a,c,d cannot be clearly separated. A broad peak is also observed around 20–30°, indicating the amorphous structure of the glass. The crystalline and microstructural properties of the obtained ZnO thin films were analysed by measuring the position, intensity and width of the peaks, which are essential for assessing the crystallite sizes. A detailed analysis of the diffractograms reveals variations in the relative intensities of individual reflections, which can be attributed to the preferential growth (with more layers) along specific crystallographic planes within the crystal. The Debye-Scherrer formula [22] was used to measure the crystallite size D:

$$D = \frac{k \cdot \lambda}{\beta \cdot \cos\theta} \tag{1}$$

where $k = 0.9$ is constant for spherical crystallite shape, λ is wavelength of X-rays (CuKα = 0.15406 nm), θ is Bragg angle of the most intense peak and β is the full width at half maximum of the peak.

Based on this formula, the crystallite size values for all the examined films were calculated from the clearest separated peak (110) in Fig. 3 and presented in Table 2. The obtained results indicate that the crystallite size increases by a very small amount with an increase in the number of layers which is similar to the data obtained by Ribut *et al.* [23]. Furthermore, the crystallites are slightly smaller in the films obtained with 2-methoxyethanol solvent as compared to the crystallites in the films grown with methanol as the solvent.

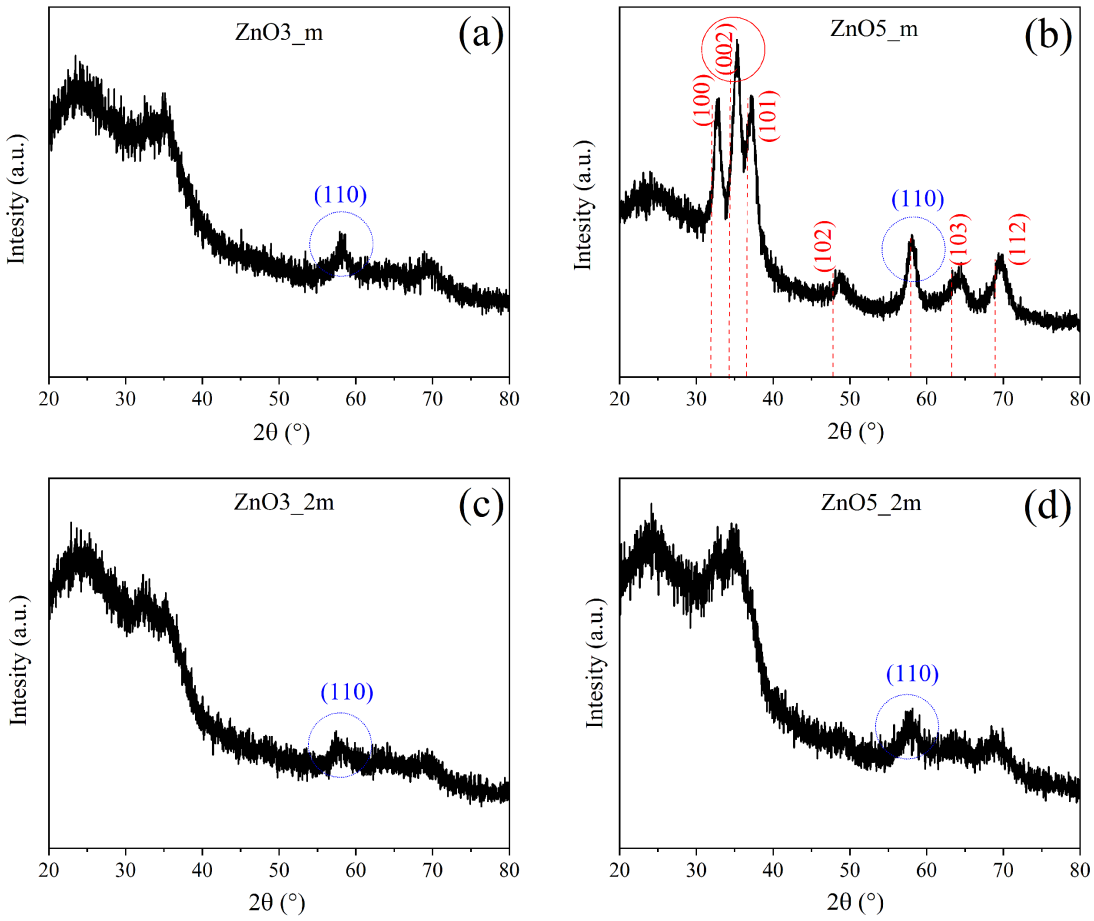

Figure 3. Diffractograms of three-layered (a) and five-layered (b) ZnO films with methanol solvent, and three-layered (c) and five-layered (d) ZnO films with 2-methoxyethanol solvent

Table 2. The crystallite size and band gap values for all the examined ZnO thin films

Film label	Crystallite size [nm]	Band gap [eV]
ZnO3_m	5.5	2.91
ZnO5_m	6.1	2.83
ZnO3_2m	4.3	3.06
ZnO5_2m	4.8	2.84

This is in accordance with the results obtained by Foo *et al.* [24].

Diffraction pattern shown in Fig. 3b indicates that the preferential growth of crystallites in the five-layered ZnO film grown with methanol occurs along the *c*-axis, as the peak around 34° diffraction angle is particularly prominent. The (002) plane is regarded as the most energetically stable with the least amount of surface free energy which was confirmed by other authors [25–27]. Based on this conclusion, we stipulate the same preferential growth in other films. The preferential crystallographic orientation can be determined from the texture coefficient (*TC*), which is calculated using the following equation [28]:

$$TC = \frac{\frac{I_{(hkl)}}{I_{r(hkl)}}}{\frac{1}{n}\sum \frac{I_{(hkl)}}{I_{r(hkl)}}} \quad (2)$$

where $I_{(hkl)}$ is the intensity of the observed peak in the measured sample, n is the number of observed peaks, and $I_{r(hkl)}$ is the reference intensity value of the peak. The texture coefficient values were calculated using this equation, but only for the five-layered ZnO thin film, as all the peaks are clearly observed in this case. The *TC* value is greater than 1 only for the (002) plane [29], confirming the preferential orientation along the *c*-axis.

The variation in optical absorption of the ZnO films with different number of layers and type of solvent is shown in Fig. 4a, where it is clearly visible that the absorption decreases from 80% to below 40% with increased wavelength of the incident light. From the image, a change in the wavelength around 370 nm can be observed, which corresponds to an electronic transition near the band edge of crystalline ZnO (3.2 eV), suggesting the possibility of an indirect transition. It is also noticeable that the absorption is lower for a smaller number of layers and methanol as the solvent. To determine the band gap width, the data obtained using the UV-Vis spectrophotometer were analysed using the Tauc method [30,31]:

$$(\alpha h\nu)^{\frac{1}{n}} = A(h\nu - E_g) \quad (3)$$

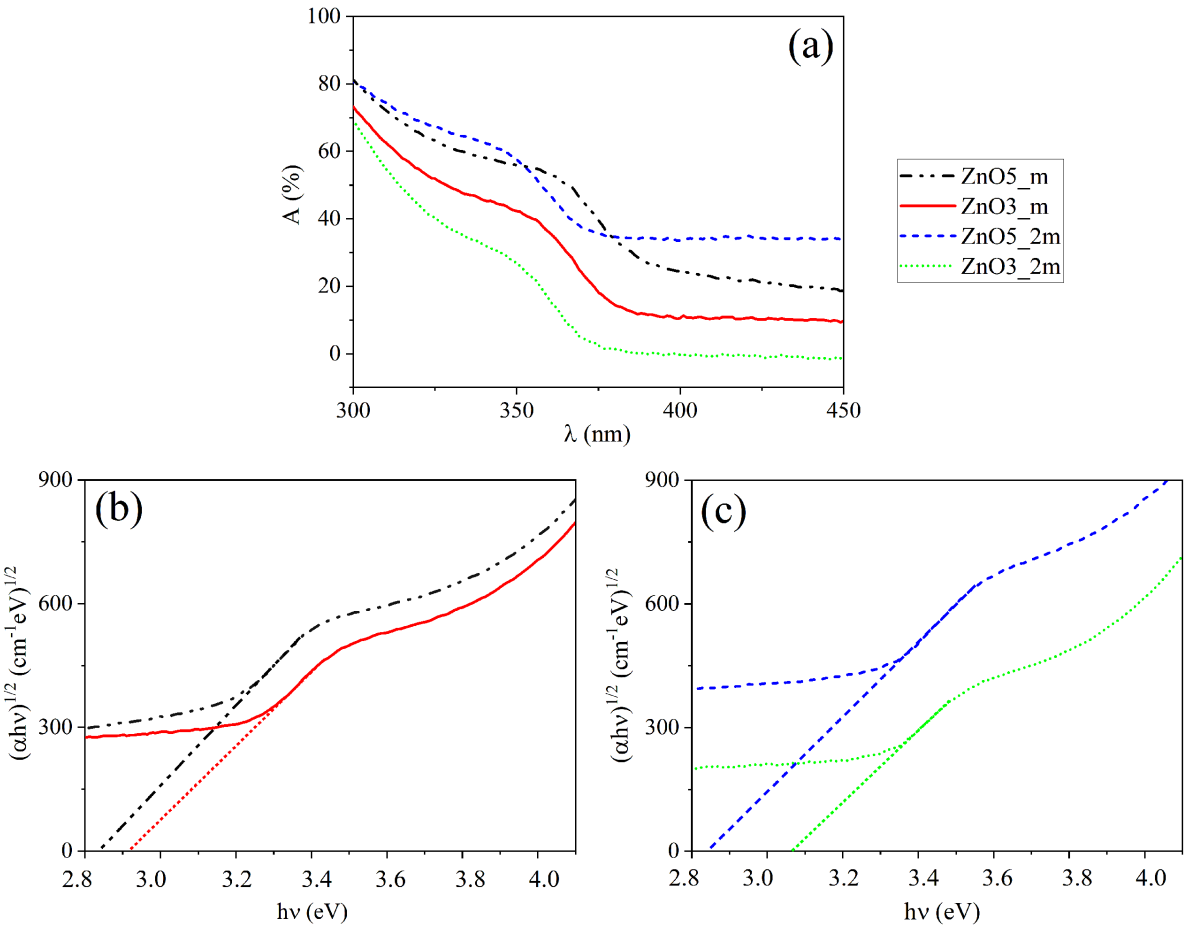

Figure 4. UV-Vis absorption spectra for three-layered and five-layered ZnO thin films created from solutions with different solvents (a) and Tauc plots for indirect transitions with methanol solvent (b) and 2-methoxyethanol (c)

where h is the Planck's constant, ν is frequency of the radiation, α is absorption coefficient, E_g is band gap energy, A is proportionality constant and n is a constant dependent on the nature of the transition. The constant n has values of 1/2 and 3/2 for direct allowed and forbidden transitions, respectively, and 2 and 3 for indirect allowed and forbidden transitions, respectively.

The linear sections of the obtained curves in the plot of $(\alpha h\nu)^{1/2}$ vs. $(h\nu)$ shown in Figs. 4b,c, were extrapolated to the x-axis [32]. The energy defined by the intersection of the line and the x-axis corresponds to the threshold energy of the incident radiation that is sufficient to excite an electron from the top of the valence band of this semiconductor to the bottom of the conduction band, or the energy corresponding to the band gap width. Electrons with energies lower than the band gap energy E_g cannot overcome the energy barrier. From this, it follows that the Tauc method is a practical way to determine the band gap width for semiconductors. However, the measurements indicated the low accuracy of this method because it is very difficult to determine whether the semiconductor is direct or indirect as, regardless of n (2 or 1/2), part of the Tauc curve is always linear [33]. An example of this are ZnO thin films on a glass substrate, which are assumed to have predominantly indirect allowed transitions due to the glass substrate's amorphous structure. In Figs. 5b,c it is clearly visible that the band gap width decreases with increasing number of layers, with a slightly smaller band gap width for ZnO thin films obtained from methanol solvent, which is a consequence of slightly larger nanoparticles and the thickness of the film itself. The data for the band gap width of the obtained ZnO thin films are shown in Table 2.

IV. Conclusions

Three-layered and five-layered ZnO films were successfully produced from a solution with different solvents (methanol and 2-methoxyethanol) on a microscope glass substrate using spin coating method. The morphological properties obtained through SEM and AFM provide information about the homogeneity of the obtained ZnO films. The thickness of the ZnO films grown from a solution with methanol as the solvent is difficult to determine with high accuracy due to the wrinkled surface. The estimated thickness of the three-layer films is 360 nm, while the thickness of the five-layer films is 100 nm greater. The ZnO films obtained from a solution with 2-methoxyethanol provide a much more homogeneous surface, with the thickness of the three-layer films being 80 nm and the five-layer films 120 nm. The roughness of the films decreases with the increase in the number of layers and it is much lower than in the ZnO films grown from the solution using methanol as the solvent.

For all the produced ZnO films, XRD analysis revealed a hexagonal wurtzite crystal structure with preferential crystal growth along the c-axis. As the number of layers increases, diffraction peaks become sharper with higher intensity, indicating a higher crystalline nature of the ZnO films. The crystallite size, calculated using the Debye-Scherrer formula, varies between 4.3 and 6.1 nm and it slightly increases with the number of layers, regardless of the solvent type, although it is slightly smaller for the 2-methoxyethanol solvent.

The analysis of the UV-Vis absorption spectrum, using the Tauc method, showed that as the number of layers increases, the band gap decreases, with a significantly smaller value observed for the ZnO thin films with methanol solvent, which is a result of the slightly larger nanoparticle size. The band gap values are smaller for all obtained ZnO thin films compared to the band gap of the bulk ZnO, which is 3.37 eV, with values ranging from 2.83 to 3.06 eV.

Acknowledgement: This work was supported by the Federal Ministry of Science and Education of the Bosnia and Herzegovina (No. 01-3840-VI-1/23) and by the Ministry of Science, Higher Education and Youth, Canton Sarajevo, Federation of Bosnia and Herzegovina, Bosnia and Herzegovina (No. 27-02-35-33087-3/24). We would like to thank Aida Smajlagić for her help with sol-gel preparation in Tuzla, Amra Salčinović Fetić for her assistance during the annealing of ZnO films in Sarajevo and Jelena Potočnik for the cross-section SEM micrographs in Belgrade.

References

1. J. Zhu, J. Zhang. H. Zhou, W. Qin, L. Chai, Y. Hu, "Microwave-assisted synthesis and characterization of ZnO-nanorod arrays", *Trans. Nonferrous Met. Soc. China*, **19** [6] (2009) 1578–1582.
2. S. Raha, M. Ahmaruzzaman, "ZnO nanostructured materials and their potential applications: progress, challenges and perspectives", *Nanoscale Adv.*, **4** [8] (2022) 1868–1925.
3. M. Samadi, M. Zirak, A. Naseri, E. Khorashadizade, A.Z. Moshfegh, "Recent progress on doped ZnO nanostructures for visible-light photocatalysis", *Thin Solid Films*, **605** (2016) 2–19.
4. M. Smirnov, C. Baban, G.I. Rusu, "Structural and optical characteristics of spin-coated ZnO thin films", *Appl. Surface Sci.*, **256** [8] (2010) 2405–2408.
5. R. Triboulet, J. Perriere, "Epitaxial growth of ZnO films", *Prog. Crystal Growth Character. Mater.*, **47** [2-3] (2003) 65–138.
6. C. Shaoqiang, Z. Jian, F. Xiao, W. Xiaohua, L. Laiqiang, S. Yanling, X. Qingsong, W. Chang, Z. Jianzhong, Z. Ziqiang, "Nanocrystalline ZnO thin films on porous silicon/silicon substrates obtained by sol–gel technique", *Appl. Surface Sci.*, **241** [3-4] (2005) 384–391.
7. A. Moustaghfir, E. Tomasella, S.B. Amor, M. Jacquet, J. Cellier, T. Sauvage, "Structural and optical studies of ZnO thin films deposited by rf magnetron sputtering: influence of annealing", *Surface Coatings Technol.*, **174** (2003) 193–196.
8. S. Blackwell, R. Smith, S.D. Kenny, J.M. Walls, C.F. Sanz-

Navarro, "Modelling the growth of ZnO thin films by PVD methods and the effects of post-annealing", *J. Phys. Condensed Matter*, **25** [13] (2013) 135002.
9. M. Purica, E. Budianu, E. Rusu, M. Danila, R. Gavrila, "Optical and structural investigation of ZnO thin films prepared by chemical vapor deposition (CVD)", *Thin Solid Films*, **403** (2002) 485–488.
10. A.J.C. Fiddes, K. Durose, A.W. Brinkman, J. Woods, P.D. Coates, A.J. Banister, "Preparation of ZnO films by spray pyrolysis˝, *J. Crystal Growth*, **159** [1-4] (1996) 210–213.
11. M. Sahal, B. Hartiti, A. Ridah, M. Mollar,B. Marí, "Structural, electrical and optical properties of ZnO thin films deposited by sol-gel method", *Microelectron. J.*, **39** [12] (2008) 1425–1428.
12. V. Kumar, N. Singh, R.M. Mehra, A. Kapoor, L.P. Purohit, H.C. Swart, "Role of film thickness on the properties of ZnO thin films grown by sol-gel method", *Thin Solid Films*, **539** (2013) 161–165.
13. A. Modrić-Šahbazović, I. Gazdić, A. Smajlagić, E. Karić, L. Babajić, L. Dedić, "Comparison of different self-assembly methods for formation of a homogenous monolayer of polystyrene", *J. Phys. Conference Series*, **2930** [1] (2024) 012007.
14. M. Khiari, M Gilliot, M Lejeune, F Lazar, A Hadjadj, "Preparation of very thin zinc oxide films by liquid deposition process: Review of key processing parameters", *Coatings*, **12** [1] (2022) 65.
15. K.L. Chopra, P.D. Paulson, V. Dutta, "Thin film solar cells: An overview", *Prog. Photovoltaics*, **12** [2-3] (2004) 69–92.
16. Y. Sun, L. Chen, Y. Bao, Y. Zhang, J. Wang, M. Fu, J. Wu, D. Ye, "The applications of morphology controlled ZnO in catalysis", *Catalysts*, **6** [12] (2016) 188.
17. Y. Aoun, B. Benhaoua, B. Gasmi, S. Benramache, "Study the structural, optical and electrical properties of sprayed zinc oxide (ZnO) thin films before and after annealing temperature", *Main Group Chem.,* **14** [1] (2015) 27–33.
18. S.J. Kwon, J.H. Park, J.G. Park, "Wrinkling of a sol-gel-derived thin film", *Phys. Rev. E*, **71** [1] (2005) 011604.
19. S.S. Shariffudin, M.H. Mamat, S.H. Herman, M. Rusop, "Characteristics of layer-by-layer ZnO nanoparticles thin films prepared with different deposition layer", pp. 899-902 in *2012 IEEE Symposium on Humanities, Science and Engineering Research*, Kuala Lumpur, Malaysia, 2012.
20. M. Toubane, R. Tala-Ighil, F. Bensouici, M. Bououdina, W. Cai, S. Liu, M. Souier, A. Iratni, "Structural, optical and photocatalytic properties of ZnO nanorods: Effect of aging time and number of layers", *Ceram. Int.*, **42** [8] (2016) 9673–9685.
21. ICDD Card No. 36-1451 (ZnO), International Center for Diffraction Data.
22. B.D. Cullity, *Elements of X-ray Diffraction*, Addison. Wesley Mass, 1978, pp. 127-131.
23. S.H. Ribut, C.A.C. Abdullah, M.Z.M. Yusoff, "Investigations of structural and optical properties of zinc oxide thin films growth on various substrates", *Results Phys.*, **13** (2019) 102146.
24. K.L. Foo, M. Kashif, U. Hashim, W.W. Liu, "Effect of different solvents on the structural and optical properties of zinc oxide thin films for optoelectronic applications", *Ceram. Int.*, **40** [1] (2014) 753–761.
25. D. Aryanto, W.N. Jannah, T. Sudiro, A.S. Wismogroho, P. Sebayang, P. Marwoto, "Preparation and structural characterization of ZnO thin films by sol-gel method", *J. Phys. Conference Series*, **817** [1] (2017) 012025.
26. N.B. Patil, A.R. Nimbalkar, M.G. Patil, "ZnO thin film prepared by a sol-gel spin coating technique for NO_2 detection". *Mater. Sci. Eng. B*, **227** (2018) 53–60.
27. I.A. Elsayed, A.S. Afify, "Controlling the surface morphology of ZnO nano-thin film using the spin coating technique", *Materials*, **15** [17] (2022) 6178.
28. D. Aryanto, P. Marwoto, T. Sudiro, M.D. Birowosuto, Sugianto, Sulhadi, "Structure evolution of zinc oxide thin films deposited by unbalance DC magnetron sputtering", *AIP Conf. Proc.*, **1729** (2016) 020039.
29. B. Zhu, X. Cai, M. Xie, X. Shi, "Structure, electrical and optical properties of ZnO and Cu-doped ZnO films prepared by magnetron sputtering at different H_2 fluxes", *Process. Appl. Ceram.*, **18** [2] (2024) 130–145.
30. J. Klein, L. Kampermann, B. Mockenhaupt, M. Behrens, J. Strunk, G. Bacher, "Limitations of the Tauc plot method", *Adv. Funct. Mater.*, **33** [47] (2023) 2304523.
31. P. Makuła, M. Pacia, W. Macyk, "How to correctly determine the band gap energy of modified semiconductor photocatalysts based on UV-Vis spectra", *J. Phys. Chem. Lett.*, **9** [23] (2018) 6814–6817.
32. R. Raciti, R. Bahariqushchi, C. Summonte, A. Aydinli, A. Terrasi, S. Mirabella, "Optical bandgap of semiconductor nanostructures: methods for experimental data analysis", *J. Appl. Phys.,* **121** (2017) 234304.
33. P.H. Andrade, C. Volkringer, T. Loiseau, A. Tejeda, M. Hureau, A. Moissette, "Band gap analysis in MOF materials: Distinguishing direct and indirect transitions using UV-vis spectroscopy", *Appl. Mater. Today* **37** (2024) 102094.